SIZE DEPENDENCE OF MECHANICAL PROPERTIES OF GOLD AT THE MICRON SCALE

JULIA R. GREER[1], WARREN C. OLIVER[2] & WILLIAM D. NIX[1]
1.Department of Materials Science and Engineering
Stanford University, Stanford, CA 94305-2205
2. MTS Nano Instruments Inc., Oak Ridge, TN 37830

ABSTRACT

The classical laws of materials science and mechanics hold that the mechanical properties of materials are independent of sample size; however the results of both experiments and molecular dynamics simulations indicate that crystalline materials exhibit strong size effects at the micron scale and below. In experimental studies, the observed size effect can be explained in terms of plastic strain gradients and the hardening effects of the associated geometrically necessary dislocations. By contrast, the atomistic simulations suggest that plastic deformation is intrinsically inhomogeneous, that the yield strength depends on the sample size even in the absence of strain gradients, and that for small single crystals, the yield strength scales with the *surface area-to-volume* ratio of the sample. These different views call for studies of the mechanical properties of small crystals without significant strain gradients.

Results of uniaxial compression experiments on gold at the micron scale, without significant stress/strain gradients, are presented. Two unique fabrication processes are used to create single-crystalline and polycrystalline Au free-standing cylinders with sub-micron dimensions. These tiny cylinders are then tested in uniaxial compression using the MTS Nanoindenter with a custom-machined flat punch diamond tip. Stress, strain, and instantaneous stiffness of the pillars are measured and the compressive stress and strain are determined from these quantities. Test results indicate a significant increase in flow stress, up to several GPa, as the pillars are compressed. Although there appears to be a significant increase in flow stress with decreasing sample size, a physical model for this has not been developed. At the time of this writing, we are not certain of the cause of the high strengths observed. Several possibilities, including the development of ultra-fine dislocation substructures, the creation of stacking faults and the strain hardening of small crystals by dislocation starvation are all briefly discussed.

1 INTRODUCTION

Systematic investigations of the characteristic length scales associated with the widely observed increase in strength with decreasing sample size date back to 1994 when Fleck et al. [1] described a series of experiments on yielding of copper wires in tension and torsion and observed higher flow stresses for smaller-diameter wires when tested in torsion compared to tension. The ideas in their paper initiated a burst of experimental studies on size-dependent mechanical properties. Stolken and Evans [2] reported higher strengths for thinner Ni foils subjected to the same bending conditions as thicker ones. Results of nanoindentation experiments in 1993 [3-4] showed a very strong inverse relationship between the hardness and the indentation depth or size of the indentation. The one similarity among these experimental studies is the presence of strain gradients in the deformation process. In nanoindentation experiments, for example, plastic deformation is confined within a very small volume. This results in the creation of non-uniform stresses and strains within the sample, thereby setting up strong gradients of strain, which are thought to be responsible for the so-called indentation size effect (ISE) [5-6].

Along a different line, Baskes and his colleagues (Gerberich et al. [7] and Horstemeyer et al. [8]) investigated plasticity at the atomic scale by employing the Embedded Atom Method (EAM) to calculate flow stresses resulting from shearing a computational unit cell with a specified number of atoms, initially in a perfect crystalline array. They too found higher yield strengths for smaller samples. They concluded that plastic deformation is intrinsically inhomogeneous, that the

yield strength depends on the sample size even in the absence of strain gradients, and that for small single crystals, the yield strength scales inversely with the *surface area-to-volume* ratio of the sample.

This brief review shows that there are at least two rather different approaches that have been developed to explain the observation of higher strengths in smaller volumes of material. In one set of explanations, the higher strengths are linked to the strong gradients of strain that accompany deformation is such small volumes. In the other approach, the high strengths are associated the dislocation starved conditions that prevail in small volumes, causing the nucleation of dislocations to dominate the plastic resistance. One way to shed light on this problem would be to mechanically test small volumes of crystalline material without strong gradients of plastic strain. Here we describe the results of a series of experiments involving uniaxial deformation of very small volumes of gold.

2 MICRON SCALE DEFORMATION WITHOUT STRAIN GRADIENTS

In order to gain insight into the deformation mechanisms responsible for plasticity at the micron scale, we have designed and executed experiments for testing the elastic and plastic properties of gold *in the absence of* the strong gradients of strain usually associated with micron scale deformation. The test methodology includes the fabrication of single-crystalline and polycrystalline free-standing gold cylinders (pillars) of sub-micron dimensions using two distinct fabrication processes. The uniaxial deformation properties of these pillars are studied via micro-compression testing techniques, following the approach of Uchic et al. [9]. As described below, we have developed both a focused ion beam (FIB) machining technique and an IC fabrication process for creating sub-micron sized pillars of gold. We have also developed uniaxial testing techniques for studying the mechanical properties of these tiny samples. We are able to conduct uniaxial compression tests on pillars of varying sizes and aspect ratios using the MTS Nanoindenter XP with a custom-machined flat punch diamond tip.

3 FABRICATION PROCESSES

We have developed two distinct fabrication processes for sample manufacturing. The first employs the Focused Ion Beam (FIB) to etch patterns of interest in gold films and in single crystal gold discs while the second utilizes the Stanford Nanofabrication Facility (SNF) for lithography-governed processing. In the *Focused Ion Beam Fabrication Approach*, a wafer is first coated with a 10nm thick layer of Ti to serve as a sticking layer, and this is followed by the evaporation of a 250 nm-thick gold film, without breaking the vacuum. Additional gold is electrodeposited on top of the existing gold film up to the thickness of 3μm and annealed at 600^{o}C for 5 hours. This typically results in a 3μm-tall columnar grain structure with each grain varying between 3μm and 6μm in diameter. The crystals created by FIB-ing pillars from these films are <111> oriented. Alternatively, a <001>-oriented single crystal gold disc is used as a precursor for pillar fabrication. A high current of Ga ions of 3000pA in the FIB is then used to mill out a donut-shaped area in the film leaving a 4μm -diameter “island” in the center. It is important to fabricate the pillar in a crater to guarantee that the indenter tip is in contact only with the pillar of interest. Finer currents and tilt angles are then used to refine this structure into a 3:1 aspect ratio upright gold pillar with a flat top. A representative example of a FIB’d gold pillar is shown in Fig. 1.

In the *Microfabrication Approach*, 250nm of Ti/TiN is sputter-deposited onto the wafer to serve as a conductive yet non-reflective layer for further processing. Then a 3μm-thick layer of photoresist is spun onto the wafer, baked, and exposed in the Nikon G-line stepper. We designed a mask pattern to image isolated contact holes ranging from 0.8μm to 1.2μm in diameter while maintaining small separation distances between the contact holes for better proximity correction. After the post-exposure bake, the contact holes are developed and dry etched in O_2 plasma to

enhance straight wall uniformity. The gold is then electrodeposited into the holes from the revealed TiN circles and the photoresist is subsequently removed. Some examples of the electroplated pillars are shown in Fig. 2.

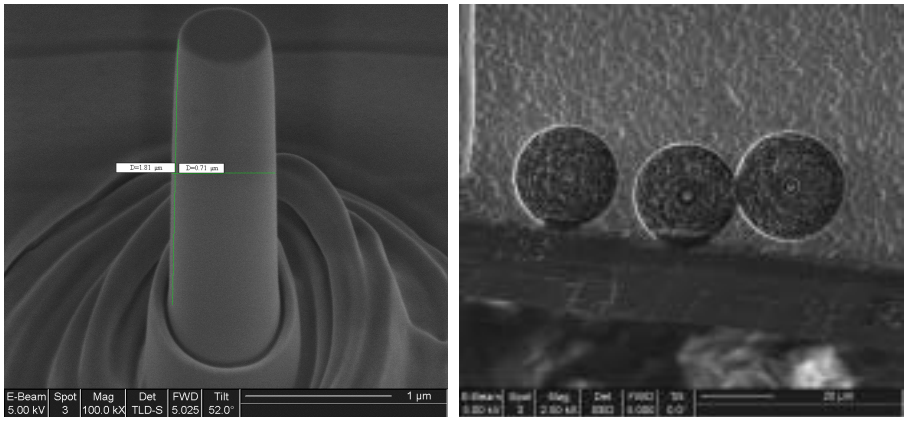

Figure 1: (a) FIB image of free-standing gold pillar, 710 nm in diameter and 2300 nm tall. The pillar was machined from a <001> gold crystal. (b) Top view of the "Donut Holes."

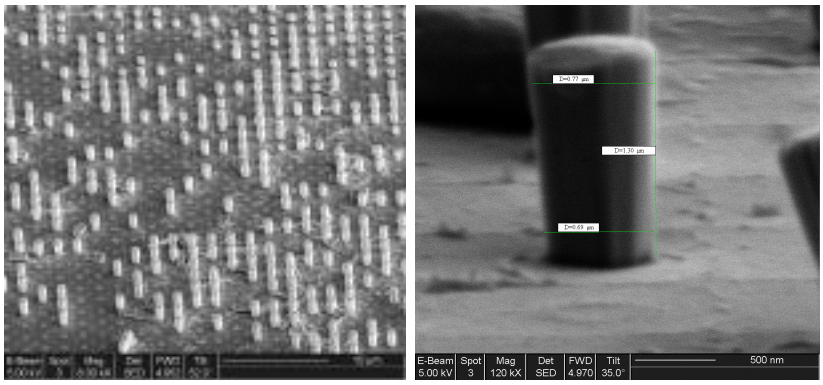

Figure 2: (a) SEM image of an array of free-standing electroplated gold pillars at 52^{o} Tilt, (b) Single pillar: 730 nm in diameter and 2170 nm tall.

4 EXPERIMENTAL PROCEDURE

All pillars were compressed using the Nanoindenter XP with a flat punch indenter tip. The flat punch tip was custom machined out of a standard Berkovich indenter by etching off the tip in the FIB. Most experiments were performed using multiple cycles of loading/unloading before reaching the maximum load in order to ensure that the unloading data was indeed elastic. In each experiment, the indenter was loaded and unloaded at least twice while maintaining a constant strain rate of $0.004s^{-1}$, with each of the unloadings terminated at 10% of the hold load to ensure the presence of the contact. Load-displacement data were collected in the Continuous Stiffness Measurement (CSM) mode using the DCM module of the instrument. The load-displacement data obtained during the compression experiments were then converted to stresses and strains assuming that the plastic volume of the cylindrical sample is preserved during deformation.

5 COMPRESSION OF GOLD PILLARS – SIZE EFFECTS

The results of our uniaxial compression experiments indicate a strong sample size effect: pillars made by both fabrication methods yield at stresses that are much higher than the typical yield strength of bulk gold which is ≈50MPa. A stress-strain curve for a pillar that had been machined from a <001> gold single crystal is shown in Fig. 3. The shape of the stress strain curve is as expected and both the initial loading slope and the unloading slopes compare favorably with the elastic modulus of gold in the <001> direction (186GPa). However, the flow stress reached after 15-20% strain is nearly 2GPa, much higher than would be expected for pure gold. To ensure that the diamond indenter was actually resting on the gold pillar only we have compared the measured stiffness with that expected for the compression of these gold pillars. This too is shown in Fig. 3. Near the end of the test the measured stiffness is close to that expected. This provides strong evidence that only the pillar was being compressed in this experiments and that the high compressive strengths shown in Fig. 3 are not in error. The gradual rise is stiffness with increasing displacement shown in Fig. 3 is thought to be due to asperities or a slight misalignment of the sample relative to the flat face of the indenter.

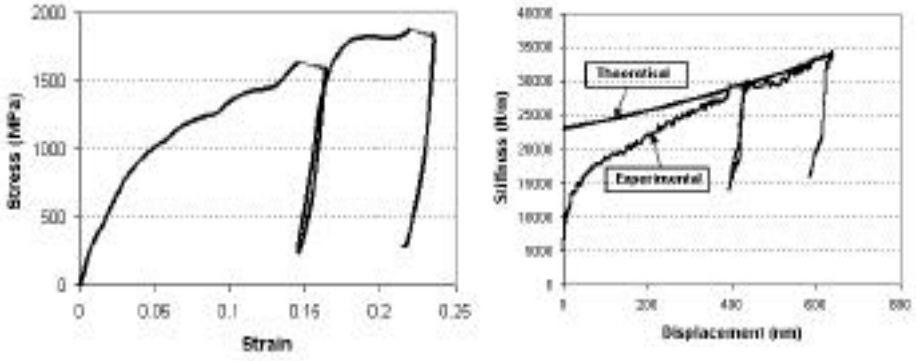

Figure 3: (a) Stress-strain behavior of an <001>-oriented gold pillar created by FIB machining. (b) The stiffness plot shows the measured stiffness compared to the expected stiffness for this gold pillar.

SEM analysis indicates that all pillars deformed by crystallographic slip on {111}-type planes, as expected. Images representing the same pillar before and after deformation are shown in Fig. 4. The slip lines on the deformed specimen are oriented at approximately 55^{o} from the loading axis, matching the calculated value of 54.7^{o} as the angle between <001> and <111> zone axes.

The pillars made by electroplating also yielded at stresses much higher than expected for bulk gold. Figure 5 shows a comparison of the stress-strain behavior for an electroplated pillar compared with the properties of a similarly sized pillar machined from the <001> single crystal (Fig. 3). The compressive flow properties are similar. The measured stiffness vs. displacement is also compared with the expected stiffness for the electroplated pillar. The approximate agreement in the stiffness again indicates that the diamond indenter was making contact with the gold pillar only and that the high compressive stresses in the electroplated pillars are not in significant error.

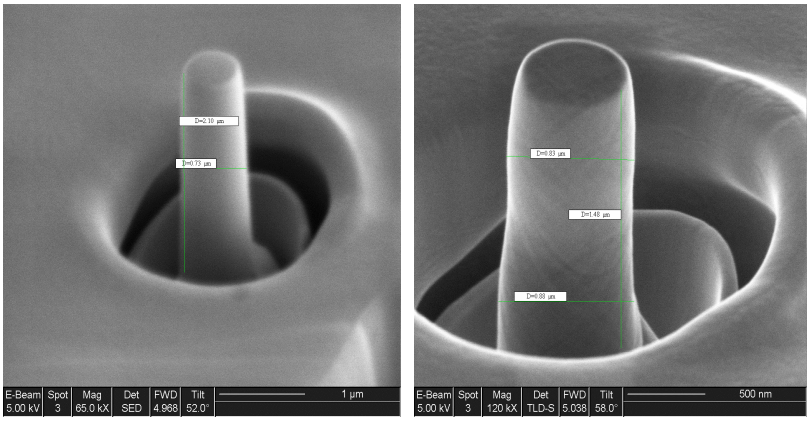

Figure 4: SEM images of (a) undeformed and (b) deformed pillar. Slip lines are present in the deformed pillar.

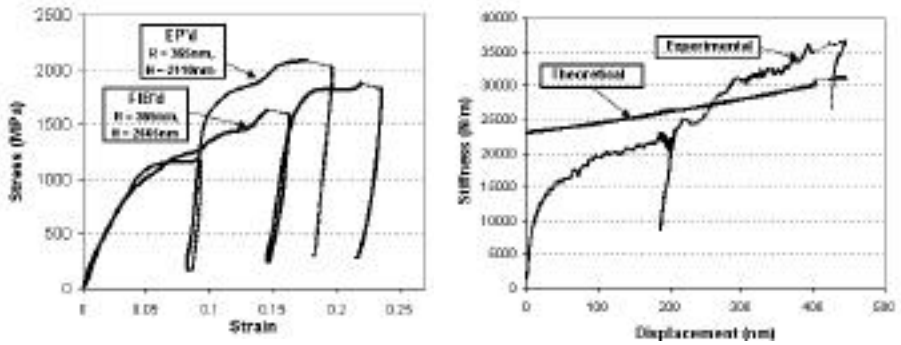

Figure 5: Comparison of the stress-strain curves for as-deposited electroplated and FIB'd pillars.

6 DISCUSSION

The results of all of our experiments indicate that a distinct size effect is present when sub-micron-sized gold pillars are plastically deformed in uniaxial compression. The samples fabricated out of single-crystal gold reach axial stresses corresponding to a significant fraction of the theoretical shear strength of gold (axial stress $\sigma_{th} \approx 10$GPa). We believe this effect is not due to Ga implantation into the surface of the gold during FIB processing. Arnold, et al. [10] and Machalett, et al. [11] independently demonstrated that surface damage from a 30KeV Ga^{+} beam on FIB-prepared TEM specimens of gold penetrated no further than 20-25nm into the surface when the Ga beam is directed normal to the surface. Less penetration is expected when the Ga ions strike the sides of the pillars at low angles of incidence. Even if some damage were present at the surface, it could hardly explain the huge flow stresses we have observed. Even quite refractory metallic glasses rarely have strengths greater than 2GPa. Furthermore, our compression tests on pillars fabricated by electroplating give similar flow stresses, as shown in Figure 5.

At present we do not understand why these small pillars are as strong as they are. If these pillars are strengthened by ordinary dislocation substructures, the average dislocation spacing would have to be less than 10 nm and the cell size would be in the range of 100 nm. Given the proximity of free surfaces in these small pillars and the tendency for dislocations to leave the

crystal, such substructure hardening seems unlikely. Another possibility is that plastic flow might involve the nucleation and motion of partial dislocations, which leave stacking faults in the crystal as they glide. A significant flow resistance would develop as subsequent partial dislocations would be forced to intersect with these faults. Such an account would naturally explain the gradual hardening observed. TEM studies underway now will indicate whether either of these possibilities should be pursued.

Another possible explanation for these high strengths involves the concept of dislocation starvation. In ordinary plasticity dislocation motion leads to dislocation multiplication by such processes as double cross-slip. This invariably leads to dynamic softening before strain hardening occurs through the elastic interactions of dislocations. For bulk metals these processes eventually lead to strong Taylor hardening. However, dislocations in small crystals, unlike in bulk samples, travel much smaller distances before reaching the free surface and annihilating there, thereby reducing the probability of multiplication. Indeed, Gilman's description of dislocation multiplication leads naturally to a length scale for dislocation multiplication, δ, the distance a dislocation must travel before it creates another. This multiplication constant can be of the order of one micron. This suggests that crystals smaller than this characteristic length might behave quite differently from bulk crystals. If the characteristic length for multiplication is larger than the crystal size, then dislocations would leave the crystal faster than they multiply, leading eventually to dislocation starvation. Once the crystal becomes dislocation starved, new dislocations would need to be nucleated, either at free surfaces or in the bulk, for continued plastic deformation. This would require very high stresses and would lead to very high strengths.

The proposed dislocation starvation model has not been fully developed at this point. Current efforts are focused on the preparation of TEM samples of the pillars before and after the deformation and observing the evolution of dislocations inside. This will provide much needed guidance for the modeling of these unusual strength effects.

7 REFERENCES

1. Fleck, N.A., Muller, G.M., Ashby, M.F. and Hutchinson, J.W., Acta metall. mater., vol.42, 475 (1994).
2. Stolken, J.S. and Evans, A.G., Acta mater., vol.46, 5109 (1998).
3. Stelmashenko, N.A., Walls, M.G., Brown, L.M. and Millman, Y.V., Acta metall. mater., vol.41, 2855 (1993).
4. De Guzman, M.S., Neubauer, G., Flinn, P. and Nix, W.D., Mater. Res. Symp. Proc., vol.308, 613 (1993).
5. Nix, W.D. and Gao, H., J. Mech. Phys. Solids, vol.46, 411 (1998).
6. Gao, H., Huang, Y., Nix, W.D. and Hutchinson, J.W., J. Mech. Phys. Solids, vol.47, 1239 (1999).
7. Gerberich, W.W, Tymiak, N.I., Grunlan, J.C., Horstemeyer, M.F., and Baskes, M.I Journal of Applied Mechanics – Tranactions of ASME, vol.69, 433-442 (2002).
8. Horstemeyer, M.F., Baskes, M.I., and Plimpton, S.J., Acta Materialia, vol.49, 4363-4374 (2001).
9. Uchic, MD, Dimiduk, D.M., Florando, J.N. and Nix, W.D., Science, vol.305, 986-989 (2004).
10. Arnold, B., Lohse, D., Bauer, H., Gemming, T., Wetzig, K., and Binder, K., Microsc. Microanal., vol.9, 140 (2003).
11. Machalett, F., Edinger, K., Melngailis, J., Diegel, M., Steenbeck, K., Steinbeiss, E., Appl. Phys. A, vol.71, 331-335 (2000).